

<https://helda.helsinki.fi>

---

## Chemical Characterization of Gas- and Particle-Phase Products from the Ozonolysis of alpha-Pinene in the Presence of Dimethylamine

Duporte, Geoffroy

2017-05-16

---

Duporte , G , Riva , M , Parshintsev , J , Heikkinen , E , Barreira , L M F , Myllys , N ,  
Heikkinen , L , Hartonen , K , Kulmala , M , Ehn , M & Riekkola , M-L 2017 , ' Chemical  
Characterization of Gas- and Particle-Phase Products from the Ozonolysis of alpha-Pinene  
in the Presence of Dimethylamine ' , Environmental Science & Technology , vol. 51 , no. 10 ,  
pp. 5602-5610 . <https://doi.org/10.1021/acs.est.6b06231>

---

<http://hdl.handle.net/10138/318935>

<https://doi.org/10.1021/acs.est.6b06231>

---

acceptedVersion

---

*Downloaded from Helda, University of Helsinki institutional repository.*

*This is an electronic reprint of the original article.*

*This reprint may differ from the original in pagination and typographic detail.*

*Please cite the original version.*

# Chemical Characterization of Gas- and Particle-Phase Products from the Ozonolysis of $\alpha$ -Pinene in the Presence of Dimethylamine

*Geoffroy Duporté,<sup>†</sup> Matthieu Riva,<sup>‡</sup> Jevgeni Parshintsev,<sup>†</sup> Enna Heikkinen,<sup>†</sup> Luís M. F. Barreira,<sup>†</sup>  
Nanna Myllys,<sup>‡</sup> Liine Heikkinen,<sup>‡</sup> Kari Hartonen,<sup>†</sup> Markku Kulmala,<sup>‡</sup> Mikael Ehn,<sup>‡</sup> and Marja-  
Liisa Riekkola<sup>\*†</sup>*

<sup>†</sup> Laboratory of Analytical Chemistry, Department of Chemistry, P.O. Box 55, 00014 University of  
Helsinki, Finland

<sup>‡</sup> Division of Atmospheric Sciences, Department of Physics, P.O. Box 64, 00014 University of  
Helsinki, Finland

## 12 ABSTRACT

13 Amines are recognized as key compounds in new particle formation (NPF) and secondary organic  
14 aerosol (SOA) formation. In addition, ozonolysis of  $\alpha$ -pinene contributes substantially to the  
15 formation of biogenic SOAs in the atmosphere. In the present study, ozonolysis of  $\alpha$ -pinene in  
16 presence of dimethylamine (DMA) was investigated in a flow tube reactor. Effects of amines on SOA  
17 formation and chemical composition were examined. Enhancement of NPF and SOA formation was  
18 observed in presence of DMA. Chemical characterization of gas- and particle-phase products by high-  
19 resolution mass spectrometric techniques revealed the formation of nitrogen containing compounds.  
20 Reactions between ozonolysis reaction products of  $\alpha$ -pinene, such as pinonaldehyde or pinonic acid,  
21 and DMA were observed. Possible reaction pathways are suggested for the formation of the reaction  
22 products. Some of the compounds identified in the laboratory study were also observed in aerosol  
23 samples ( $\text{PM}_{10}$ ) collected at the SMEAR II station (Hyytiälä, Finland) suggesting that DMA might  
24 affect the ozonolysis of  $\alpha$ -pinene in ambient conditions.

## 25 INTRODUCTION

26 Atmospheric particles are known to have a significant influence on global climate  
27 change, regional air quality and human health.<sup>1-3</sup> They can be directly emitted by anthropogenic or  
28 natural sources (primary aerosols), such as wood burning and fossil fuel combustion. However, a  
29 significant fraction of atmospheric aerosol is organic in nature and often dominated by secondary  
30 organic aerosols (SOAs) formed from the oxidation of volatile organic compounds (VOCs).<sup>4-5</sup>  
31 Although SOAs contribute to a major mass fraction of ambient fine particle matter (PM<sub>2.5</sub>), current  
32 models continue to under-predict the SOA mass observed during field measurements. In addition,  
33 uncertainties remain in the chemical processes governing the SOA formation and aging.  
34 Understanding the potential species driving SOA formation and aging is therefore critical for the  
35 prediction of aerosol impact on climate change and human health.

36 Amines, ubiquitous in the atmosphere, are emitted into the atmosphere by a large variety  
37 of anthropogenic and natural sources. Globally, animal husbandry, combustion processes and  
38 industry are the main anthropogenic sources while oceans, vegetation and soils represent the main  
39 natural sources.<sup>6</sup> Ge *et al.*<sup>6</sup> have identified more than 150 atmospheric amines emitted from either  
40 anthropogenic or natural sources in the atmosphere. Low-molecular weight aliphatic amines, such as  
41 methylamine (MA), dimethylamine (DMA), trimethylamine (TMA) or ethylamine (EA), are the most  
42 abundant amines in the atmosphere. For instance, Kieloaho *et al.*<sup>7</sup> have reported that the combined  
43 concentration of the major alkylamines (EA and DMA) in the boreal forest in southern Finland is  
44 around 150 pptv. DMA has been also detected as a major alkyl amine species in particles and cloud  
45 water in semi-arid and coastal regions.<sup>8</sup>

46 Amines are highly reactive species and they are expected to play a key role in new  
47 particle formation (NPF) and SOA formation.<sup>6,9-12</sup> For instance, they are more likely to enhance NPF  
48 than ammonia (NH<sub>3</sub>).<sup>9, 13-14</sup> Therefore, understanding the transformation and fate of amines and/or

49  $\text{NH}_3$  is currently one of the main challenges in the field of atmospheric chemistry. Other laboratory  
50 studies have demonstrated that amines considerably enhance nucleation of the sulfuric acid-water  
51 system.<sup>10, 15-16</sup> Indeed, Almeida *et al.*,<sup>9</sup> showed that a few ppt of DMA enhance the aerosols formation  
52 rates of sulfuric acid by several orders of magnitudes. Evidence for the participation of amines in gas  
53 and/or multiphase chemistry has also been demonstrated.<sup>10, 17-19</sup> Recent studies have suggested that  
54 carbonyl compounds such as glyoxal,<sup>20</sup> methylglyoxal,<sup>21</sup> glycoaldehyde,<sup>20</sup> acetaldehyde<sup>20</sup> or  
55 pinonaldehyde<sup>22</sup> are able to react in aerosol phase or bulk aqueous solution with small amines. The  
56 resulting nitrogen (N)-containing compounds could then participate in SOA growth due to their low  
57 vapor pressures. In addition, Stropoli and Elrod<sup>23</sup> have reported potential multiphase reactions  
58 between amines and epoxides, which could further contribute to SOA formation. A previous  
59 experimental study has shown that the saturation vapor pressures of alkylammonium carboxylates are  
60 lower than those of their organic acid precursors, likely explaining that alkylamine neutralization by  
61 carboxylic acid enhances SOA formation.<sup>24</sup> In addition, a recent study has also shown that alkylamine  
62 neutralization of carboxylic acids also enhanced the particle hygroscopicity and the cloud  
63 condensation nuclei (CCN) activity.<sup>25</sup> It is worth nothing that, Mäkelä *et al.*<sup>17</sup> have observed that  
64 DMA concentrations were 30 times higher in aerosol samples collected during NPF events than those  
65 in non-event samples in the boreal forest at Hyytiälä Forestry Field Station in Finland. Likewise,  
66 Smith *et al.*,<sup>18</sup> have reported that aliphatic amines contributed to 23 % of the positive ions detected  
67 during NPF events at the same boreal forest site, and to 47 % at an urban site in Tecamac, Mexico.  
68 Finally, Tao *et al.*<sup>12</sup> have revealed that the heterogeneous uptake of amines is dominated by the acid-  
69 base reaction mechanism, which may contribute to particle growth in NPF events.

70 In this context, the aim of this work was to improve our understanding of amine  
71 chemistry in the atmosphere and to assess their contribution to NPF and SOA growth. Since  
72 ozonolysis of  $\alpha$ -pinene contributes substantially to the formation of biogenic SOAs in the atmosphere,  
73 its reaction was investigated in the presence of DMA in a flow tube reactor to evaluate the effect of

amines on SOA formation and chemical composition. Gas-phase products were characterized using an Aerodyne high-resolution time-of-flight chemical ionization mass spectrometer (HR-ToF-CIMS) equipped with iodide reagent ion chemistry. Aerosol size distribution was measured with a differential mobility particle sizer (DMPS). In addition, gas- and particle-phase samples collected from flow tube experiments were analyzed by ultra-high-performance liquid chromatography coupled to electrospray ionization orbitrap mass spectrometry (UHPLC-HRMS). To confirm the relevance of the laboratory findings to the ambient atmosphere, aerosol samples (PM<sub>1</sub>) were collected from the SMEAR II boreal forest site at Hyytiälä, Finland, during May–June 2016 and analyzed by the same off-line analytical methodologies. Quantum chemistry calculations were also used for the clarification of enamine formation from pinonaldehyde and dimethylamine.

## EXPERIMENTAL SECTION

**Flow Tube Reactor Experiments.** The ozonolysis of  $\alpha$ -pinene in the presence or absence of DMA was carried out in a borosilicate glass flow tube reactor (205 cm long, 4.7 cm i.d.). The experimental set-up is presented in Figure S1 while the initial experimental conditions are detailed in Table 1. The flow tube is operated using purified dry air at atmospheric pressure and room temperature ( $T = 293 \pm 3$  K) under laminar flow conditions.<sup>26-27</sup> The total gas flow was adjusted to 4.5 L/min resulting in a residence time of 53 s in the flow tube reactor. The purified air was generated by an air purification system (AADCO, 737 Series) that runs on compressed air and reduces concentrations of O<sub>3</sub>/NO<sub>x</sub> and non-methane hydrocarbons to less than 1 ppb and 5 ppb, respectively. In experiments E1-E3, 100-120 ppb (Table 1) of O<sub>3</sub> was generated by an ozone generator (Dasibi 1008-PC) and injected into the flow tube. When the ozone concentration, determined by an ozone analyzer (Thermo Scientific model 49), was stable,  $\sim 5$  ppm of  $\alpha$ -pinene was introduced into the flow tube through a mobile injector (Figure S1). The concentration of  $\alpha$ -pinene was estimated from the vapor pressure<sup>28</sup> and the measured gas flows. Finally,  $\sim 500$  ppb of DMA was introduced in the flow tube (Experiments E1'-E3') to investigate the impact of amines on the ozonolysis of  $\alpha$ -pinene. DMA (Sigma-Aldrich, 40 wt. % in

H<sub>2</sub>O) and  $\alpha$ -pinene (Sigma-Aldrich, 98 %) were generated by flushing nitrogen (N<sub>2</sub>) through the liquid compounds in glass bubblers. The DMA concentration was determined by GC-MS after solid phase micro extraction (SPME) using a SPME Arrow (Carbon WR, CTC Analytik).<sup>29</sup> Details on DMA calibration can be found elsewhere.<sup>29</sup> Aerosol size distributions were continuously measured using a differential mobility particle sizer (DMPS) in order to monitor aerosol number, surface area, and volume concentration. The different flows were controlled using mass flow controllers (MKS). All experiments were performed without an OH radical scavenger. Once aerosol volume concentration stabilized as well as the gas-phase oxidation products, aerosols were collected on filters (47 mm PTFE filters) and gaseous products on solid phase extraction (SPE) cartridges (divinylbenzene), for 1 hour at a flow rate of 1 L/min. SPE sampling was used to identify semi-volatile organic compounds in gas phase, complementary to on-line analysis by HR-ToF-CIMS. Filters and SPE cartridges were stored in dark in a freezer at – 18°C until extraction. It is worth noting, that clear memory effect was observed after switching off the injection of DMA, as it took long time to restore the initial O<sub>3</sub> concentration. Hence, to ensure reproducibility, the flow tube was cleaned between each experiments with high purity methanol (Sigma-Aldrich, HPLC grade) and flushed with clean air overnight. Methanol extracts were kept after the reactions E2' and E3' in order to study the chemical composition of the products adsorbed on the walls of the flow tube.

**Chemical Characterization of Gas- and Particle-Phase Constituents.** Real-time measurements of gas-phase oxidation products were performed with an Aerodyne high-resolution time-of-flight chemical ionization mass spectrometer (HR-ToF-CIMS), equipped with iodide (I<sup>-</sup>) reagent ion chemistry. Analyses were restricted to ions containing an iodide adduct, which guarantees detection of the parent organic compound without substantial fragmentation. Iodide-HR-ToF-CIMS has been described previously and demonstrated high sensitivity towards multifunctional oxygenated organic compounds in the gas and particle phases.<sup>30-32</sup> Characterization of N-containing compounds from the flow tube reactor experiments was performed using a Thermo Ultimate 3000 UHPLC coupled with

124 an Orbitrap Fusion TMS (Tribrid mass spectrometer) operated in positive mode. Detailed  
125 characterization of analytical procedure has previously been described.<sup>22</sup> Before extraction, an  
126 internal standard aliquot (caffeine, Sigma Aldrich, *ReagentPlus*®), controlled by gravimetry, was  
127 added to the samples. Filter samples were extracted in 7.5 mL of acetonitrile (HPLC grade, Sigma  
128 Aldrich) during 30 min of sonication at room temperature. Caffeine was used as an internal standard  
129 for semi-quantification of N-containing reaction products, due to the lack of commercially available  
130 authentic standards. Then, extracts were filtered through 0.45  $\mu$ m PTFE syringe filters (Merck  
131 Millipore Ltd.) to remove insoluble particles. The SPE samples were extracted by slowly passing 7.5  
132 mL of acetonitrile through the cartridges by vacuum. Finally, the extracts were dried under a gentle  
133 stream of nitrogen at 30 °C and reconstituted with 100  $\mu$ L of a 50/50 (v/v) mixture of acetonitrile and  
134 water (milli-Q water). Ten  $\mu$ L were injected onto the UPLC column (Phenomenex Luna Omega Polar  
135 C<sub>18</sub> column, 100  $\times$  2.1 mm, 1.6  $\mu$ m) at a flow rate of 0.6 mL/min. The eluent composition was (A)  
136 0.1 % formic acid in Milli-Q grade water and (B) 0.1 % formic acid (HPLC grade, Sigma Aldrich) in  
137 acetonitrile. The mobile phase gradient was initially 95:5 (v/v, A/B), increased to 100 % B along 15  
138 min and returned to 95:5 (v/v, A/B) in 1 min and then kept for 4 min to equilibrate the column.

139 **Ambient Samples.** Boreal forest samples were collected from May 3 to June 26, 2016 at the Station  
140 for Measuring Forest Ecosystem-Atmosphere Relations (SMEAR II) at Hyytiälä, in southern Finland  
141 (61°50.845' N, 24°17.686' E, 179 m above sea level).<sup>33</sup> The largest nearby city is Tampere, situated  
142 60 km southwest from SMEAR II with around 200 000 inhabitants. The most dominant species  
143 emitted by the forest, mainly constituted by Scots pine and Norway spruces, are  $\alpha$ -pinene and  $\Delta^3$ -  
144 carene.<sup>34</sup> Ambient aerosols were collected using a high volume sampler equipped with PM<sub>1</sub> inlet at a  
145 flow rate of 30 m<sup>3</sup>/h (Digitel DA-80) on quartz fiber filter (Sigma-Aldrich, Whatman®) with a  
146 diameter of 150 mm. Prior to sampling, quartz fiber filters were calcined at 450 °C for 6 hours to  
147 remove any possible organic contamination. Sampling was performed over a period of 12 hours (day  
148 sample, from 7 am to 7 pm and night sample, from 7 pm to 7 am). Filters were wrapped in aluminum



foil and placed in antistatic bags, which were stored at  $-18\text{ }^{\circ}\text{C}$  until extraction. In total 107 samples were collected. Filters from the field study were punched ( $31.25\text{ cm}^2$ ) and extracted using the protocol described above. Selected ion monitoring (SIM) method was applied by choosing the reaction product ions identified in the laboratory experiments. Tandem mass spectra ( $\text{MS}^2$ ) analyses were also performed to compare the  $\text{MS}^2$  fragmentation patterns of the product ions detected from ambient and laboratory samples. Field and laboratory blanks were extracted and analyzed following the same procedures to determine any potential contamination during the sampling, transportation, storage and/or analysis. The extraction efficiency for all the samples was  $94 \pm 16\%$ .

## RESULTS AND DISCUSSION

**Enhancement of NPF in the Presence of DMA.** Aerosol size distributions of SOAs formed from the ozonolysis of  $\alpha$ -pinene were continuously measured using a DMPS. As shown in Table 1, the number of particles in the experiments E1-E3 ranged from 9500 to 26000 particles per  $\text{cm}^{-3}$ . After the injection of DMA (experiment E1'-E3'), all experiments revealed a subsequent increase of the number of particles (70 000-80 000 particles per  $\text{cm}^3$ ). This clearly indicates a strong influence of DMA on SOA formation from the ozonolysis of  $\alpha$ -pinene. Such results are in agreement with observations from other laboratory studies, underlying the enhancement of NPF due to the presence of amines.<sup>9, 15, 35-37</sup> A recent theoretical study has revealed that the interaction between amines and dicarboxylic acids likely exerts a synergetic effect on NPF due to the formation of aminium carboxylate ion pairs.<sup>38</sup> As presented in Figure 1, the average median diameter of the SOAs formed from the ozonolysis of  $\alpha$ -pinene was  $20 \pm 2\text{ nm}$ , while being  $27 \pm 2\text{ nm}$  in the presence of DMA. The increase of 7 nm could be attributed to the potential reactions between organic compounds, such as aldehydes, ketones or carboxylic acids with DMA.<sup>11</sup> These reactions could lead to the formation of semi- and low- volatile organic compounds, which might further participate in the SOA formation. Therefore, to better understand the mechanisms governing the enhancement of NPF and the SOA

173 growth in the presence of DMA, chemical characterization of both gas- and particle-phase reaction  
174 products was performed.

175 **Chemical Characterization of Gaseous Reaction Products.** Gaseous reaction products were  
176 characterized by HR-ToF-CIMS. The ions selected were detected as iodide clusters ( $M + 126.9050$   
177 Da). The mass spectra of gaseous compounds identified by HR-ToF-CIMS from the ozonolysis of  $\alpha$ -  
178 pinene and the  $\alpha$ -pinene- $O_3$ -DMA reaction are presented in Figure S2. As can be seen, spectra differ  
179 significantly between both set of experiments. The subtracted mass spectrum from the experiments  
180 is shown in Figure 2, demonstrating the clear effect of DMA on the ozonolysis of  $\alpha$ -pinene. The  
181 positive values correspond to the formation of reaction products after the injection of DMA and the  
182 negative values to the depletion of products due to the presence of DMA. As shown in Figure 2, a  
183 subsequent decrease of the signal of ions attributed to pinonic ( $m/z$  311,  $C_{10}H_{16}O_3I^-$ ), pinic ( $m/z$  313  
184  $C_9H_{14}O_4I^-$ ) and hydroxy-pinonic acids ( $m/z$  327,  $C_{10}H_{16}O_4I^-$ ) were observed after the injection of  
185 DMA into the flow tube. This change can also be seen in Figure 3 especially for pinonic acid  
186 ( $C_{10}H_{16}O_3I^-$ ) whose signal dropped by a factor of  $\sim 2.5$ . In addition, depletion of highly oxidized  
187 molecules ( $m/z$  340–500 Da) previously identified in laboratory or field studies,<sup>39-41</sup> was also  
188 observed after the injection of DMA as shown in Figure 2.

189 A surprising increase of the signals of oxygenated compounds was also observed after  
190 the injection of DMA (Figures 2, 3 and S3). Figure S3 presents a mass defect plot of reaction products  
191 identified by HR-ToF-CIMS. A mass defect plot provides an effective visualization of high-resolution  
192 mass spectral data of a complex mixture in a two-dimensional way. More details about this approach  
193 can be found elsewhere.<sup>42-43</sup> As displayed in Figure S3, a large amount of gas-phase oxygenated  
194 products are formed after the injection of DMA. For example, the signal of the ion at  $m/z$  297,  
195 attributed to nor-pinonic acid ( $C_9H_{14}O_3I^-$ ), was 5 times higher in the presence of DMA. The  
196 experiments were carried out under steady-state conditions; meaning that a constant flow of reactants,  
197 oxidants and particles were continuously added to the chamber. Therefore, additional formation of

nor-pinonic acid from OH-initiated oxidation of pinonaldehyde would require additional formation of OH radicals in the system. The ozonolysis of unsaturated products arising from aldehyde-dimethylamine reaction may lead to OH radicals which could result in the formation of nor-pinonic acid. It is worth noting that the products formed from the reactions of oxygenated species with DMA exhibit a smaller carbon skeleton than the precursors, suggesting that amine chemistry induces the formation of smaller oxygenated products with a larger O/C ratio. As previously reported, pinonaldehyde is one of the major reaction product from the oxidation of  $\alpha$ -pinene.<sup>44</sup> We have recently reported the subsequent reaction of pinonaldehyde with DMA and identified the formation of N-containing compounds in both gas and particulate phases. The main gaseous products observed was an enamine ( $m/z$  196.1696 detected in positive mode -  $C_{12}H_{22}NO^+$ ).<sup>22</sup> The presence of such compounds was observed also in this work suggesting that aldehydes can react with DMA and lead to a large variety of oxygenated and/or N-containing species. It is important to note that due to the poor sensitivity of iodide ionization towards aldehydes and/or low oxidized compounds (e.g.  $C_{12}H_{21}NO$ ),<sup>30</sup> the direct observation of reactions between aldehydes and DMA was not possible here. All together 45 N-containing compounds were observed in the gas phase from the  $\alpha$ -pinene- $O_3$ -DMA reactions (e.g.  $C_6H_9NO_3$  and  $C_3H_7NO_2$ , Figure 3) by HR-ToF-CIMS (Table S1). As discussed below, the oxidation of enamine or imine arising from the reactions of carbonyl and/or carboxylic acids with DMA,<sup>11, 45</sup> might explain the large amount of the small oxygenated and N-containing compounds observed in the gas-phase.

Previous studies have reported the reactions of amines with carboxylic acids and/or carbonyl compounds in either bulk solution,<sup>20-21</sup> or aerosol phase,<sup>46</sup> and identified the formation of N-containing species. In order to investigate whether enamine formation takes place in gas or aerosol phase, we calculated the Gibbs free energies along to the reaction coordinate using the combination of density functional theory and coupled cluster methods. Detailed description of the calculations is given in Supplementary Material (Figure S4-S7, Table S2). The reaction is suggested to begin with

the formation of carbinolamine followed by subsequent dehydration leading to enamine. Calculations resulted in so high activation energy of carbinolamine formation that the bimolecular addition reaction in the atmospheric conditions is unlikely. Based on the computed Gibbs free energies the dehydration of carbinolamine is the rate-limiting step, and even the reaction is thermodynamically favourable under atmospheric conditions, the direct formation of enamine through an addition-elimination mechanism is kinetically restricted. In contrast, we investigated the stabilization effect of a single water molecule, and found that the activation energies are reduced by more than 10 kcal/mol for both addition and elimination steps. Therefore, we suggest that the reaction occurs on the molecular cluster surface. Later, enamine, formed in the aerosol phase, can evaporate to the gas phase. Also, facilitation of heterogeneous reactions by aerosol water has been shown elsewhere<sup>47</sup>.

**Ozone reduction from  $\alpha$ -pinene-O<sub>3</sub>-DMA Reaction.** As shown in Table 1, the ozone concentration dropped significantly after the addition of DMA. On average, the ozonolysis of  $\alpha$ -pinene decreased the ozone concentration from 110 ppb to 42 ppb, while the presence of DMA decreased it down to 8 ppb. The large reduction of ozone observed in these experiments cannot be solely explained by the reaction of DMA with O<sub>3</sub> or OH according to the rate constants ( $1.67 \pm 0.20 \times 10^{-18}$  and  $6.27 \pm 0.63 \times 10^{-11}$  cm<sup>3</sup>/molecule/s, respectively).<sup>48-49</sup> Further decrease is expected due to the products formed from the reaction of oxygenated species with DMA that could undergo further oxidation processes with ozone. Indeed, carbonyl groups, such as aldehydes, can react with DMA to form enamine compounds.<sup>11</sup> For instance, we have previously reported that DMA can react on the aldehyde function of pinonaldehyde and lead to carbinolamines, which then dehydrate to generate enamine compounds. In addition, formation of imines from the reaction between amines and carbonyl compounds have been observed.<sup>50</sup> Hence, ozone can react with the double bond of the enamine and/or imines species (Figure S8), leading to a primary ozonide, which decomposes to produce a Criegee biradical intermediate and a carbonyl compound. Formation of carboxylic acids can also be explained by Criegee biradical rearrangement.<sup>51</sup> As an example ozonolysis of C<sub>12</sub>H<sub>21</sub>NO is expected to lead to the

248 formation of nor-pinonaldehyde ( $C_9H_{14}O_2$ ), nor-pinonic ( $C_9H_{14}O_3$ ) and carbamic acids ( $C_3H_7O_2N$ ).  
249 A tentative reaction pathway is proposed in Figure S8, which is supported by the subsequent  
250 formation of nor-pinonic and carbamic acids after the injection of DMA (Figure 3). Other  
251 N-containing compounds, such as imines or nitroamines, may also contribute to the ozone  
252 consumption. Ge *et al.*<sup>52</sup> have identified  $CH_3N=CH_2$ ,  $(CH_3)_2NCHO$ ,  $CH_3NO_2$ ,  $CH_3N(OH)CHO$  and  
253  $CH_3NHOH$  as major products from the ozonolysis of alkylamines. Hence, ozonolysis of these  
254 N-containing species might explain the large concentration of oxygenated compounds in the gas  
255 phase. The formation of the N-containing compounds and the increase of concentration of  
256 oxygenated compounds in the gas phase can explain the enhancement of NPF and SOA growth from  
257 the ozonolysis of  $\alpha$ -pinene in the presence of DMA. It should be noted, however, that oligomerization  
258 through accretion reactions would lead to the formation of unsaturated compounds in particle phase,  
259 which could also participate in the ozone reduction. These observations suggest that amines may play  
260 an important role in the gas and heterogeneous chemistry of oxygenated species governing the SOA  
261 formation and aging.

262 **Chemical Characterization of Particulate Reaction Products.** Table 2 presents the most abundant  
263 N-containing compounds identified from the filter or the flow tube wall extract samples. These  
264 compounds were not observed without DMA in either the  $\alpha$ -pinene ozonolysis or in the laboratory  
265 blank samples. Differences between theoretical and measured masses obtained by HRMS are small  
266 and within commonly acceptable errors (i.e.,  $\pm 5$  ppm). As indicated in Table 2, the major  
267 N-containing compounds detected in particle phases are  $C_{11}H_{19}O_2N$ ,  $C_{10}H_{17}O_3N$ ,  $C_{12}H_{21}O_2N$ ,  
268  $C_{12}H_{19}O_3N$  and  $C_{13}H_{17}O_4N_3$ . Smaller N-containing compounds from 176 to 230 Da were also  
269 identified in the gas phase, by either HR-ToF-CIMS or by analysis of samples collected on SPE  
270 cartridges, demonstrating the partitioning of these compounds between gas and particle phases. High-  
271 molecular weight N-containing compounds (MW > 300 Da) were also identified. The accurate mass  
272 measurements of the corresponding  $[M + H]^+$  ions indicate the formation of  $C_{15}$ - $C_{30}$  carbon

273 compounds, presence of such compounds supports accretion reactions occurring in particle phase.  
274 Reaction between oxygenated dimers and DMA, assumed from the HR-ToF-CIMS results (Figure 2,  
275 depletion of highly oxidized molecules  $m/z$  340–500 Da) is also another hypothesis. It is worth  
276 nothing that molecules with 3 and 5 nitrogen atoms were also identified in the particle phase. They  
277 might take part in the formation of imidazole type compounds, previously observed from the reaction  
278 of glyoxal or methylglyoxal with amines in particle phase, suggesting that heterogeneous reactions  
279 should also be considered here.<sup>21, 50</sup>

280 Interestingly, as shown in Table 2, eleven N-containing compounds exhibit an identical  
281 fragment ion at  $m/z$  72.044 ( $C_3H_6ON^+$ ) in their  $MS^2$  spectra as revealed in Figure S9. Ion at  $m/z$  72 is  
282 characteristic to a tertiary amide, which is likely produced from the reaction between a carboxylic  
283 acid and DMA. This observation suggests that carboxylic acid-amine reaction is an important reaction  
284 pathway leading to specific products as discussed above. Bastanti and Pankow<sup>53</sup> have concluded that  
285 for all the acids studied (acetic, malic, maleic and pinic acids), amide formation was  
286 thermodynamically favored, supporting the hypothesis presented in this work. As for organosulfates,  
287 fragment ions at  $m/z$  80 ( $SO_3^{\bullet-}$ ), 96 ( $HSO_3^-$ ) and 97 ( $HSO_4^-$ ) are characteristic for their detection in  
288 negative ion mode,<sup>54</sup> and ion  $m/z$  72 might be a beneficial product ion for the identification of  
289 compounds arising from carboxylic acid-secondary amine reaction in positive ion mode.

290 A potential mechanism for the formation of products with a fragment ion at  $m/z$  72 is tentatively  
291 proposed in Figure S10. As an example, pinonic acid can react with DMA to form  $C_{12}H_{21}NO_2$  ( $m/z$   
292 212.164). Signal of pinonic acid decreased after the DMA addition, while product at  $m/z$  212.164  
293 increased. In contrast, nor-pinonic acid, which is tentatively proposed to be formed from the  
294 ozonolysis of  $C_{12}H_{21}NO$  (a pinonaldehyde/DMA reaction product), might further react with DMA  
295 and lead to the product ion at  $m/z$  198.149 ( $C_{11}H_{19}NO_2$ ). The  $MS^2$  spectra for the  $C_{11}H_{19}NO_2$  is given  
296 in Figure S11, and the identified fragments support the presence of an amide functional group in the  
297 structure. Hence, organic acids formed from the ozonolysis of  $\alpha$ -pinene, such as terebic, nor-pinonic,

298 terpenylic, nor-pinic, pinonic, oxopinonic and hydroxyl-pinonic acids (Figure S11), previously  
299 observed in laboratory and field studies,<sup>55-58</sup> can further react with DMA and lead to the formation of  
300 N-containing reaction products, yielding a fragment ion at  $m/z$  72 in their MS<sup>2</sup> spectra (Table 2).  
301 These results are in agreement with the results of the study of Lavi et al.<sup>24</sup> in which they observed that  
302 alkylammonium carboxylates can enhance SOA formation. Furthermore, as it has been shown by  
303 Gomez-Hernandez et al.<sup>25</sup>, alkylamine neutralization of carboxylic acids also enhances the particle  
304 hygroscopicity.

305 **Reaction Products from  $\alpha$ -pinene-O<sub>3</sub>-DMA Reaction in Ambient Aerosol.** Figure 4 presents the  
306 extracted ion chromatograms (EICs) of parent ions at  $m/z$  198.149 and 212.164 from  $\alpha$ -pinene + O<sub>3</sub>  
307 experiment (E3),  $\alpha$ -pinene + O<sub>3</sub> + DMA experiment (E3'), blank filter and PM<sub>1</sub> samples collected at  
308 Hyytiälä Forestry Field Station (23<sup>th</sup> of May, 2016). MS<sup>2</sup> fragmentation patterns of parent ion at  $m/z$   
309 198.149 and 212.164 from laboratory and field samples are shown in Figure S12.

310               Based on the excellent agreement between the retention times, the accurate masses and  
311 the MS<sup>2</sup> fragmentation pattern, parent ions at  $m/z$  198.149 (RT 4.57 min) and 212.164 (RT 5.07 min)  
312 found in the boreal forest samples were attributed to N-containing compounds formed from the  
313 oxidation of  $\alpha$ -pinene in the presence of DMA. Three other reaction products were also identified in  
314 PM<sub>1</sub> samples at the SMEAR II Station in Hyytiälä, using accurate masses. The other reaction products  
315 identified in laboratory experiments samples were not observed in the boreal forest samples. Semi-  
316 quantification was performed using caffeine as a surrogate standard, resulting in potential large  
317 uncertainties for the estimated concentrations of these products, mainly due to different extraction  
318 yields and ionization efficiency between caffeine and the analytes. However, such approach allows  
319 us to provide information on variations and time-trends that cannot be obtained otherwise. The  
320 average concentration of compounds observed at  $m/z$  198.149 was 0.161 ng/m<sup>3</sup> with a maximum  
321 concentration of 0.990 ng/m<sup>3</sup>, while it was 0.035 ng/m<sup>3</sup> for the parent ions at  $m/z$  212.164 with a  
322 maximum concentration of 0.161 ng/m<sup>3</sup>. A temporal profile of the concentration of both compounds

323 is proposed in Figure S13. The concentration of these two compounds are fairly correlated ( $r^2 = 0.46$ ),  
324 suggesting similar source of emission or formation, except from 15<sup>th</sup> of May 2016 to 20<sup>th</sup> of May  
325 2016. Even if relatively low concentration of DMA has been reported for the clean boreal forest  
326 atmosphere,<sup>7</sup> the identification of these two compounds in ambient samples suggests that DMA may  
327 have an effect on the ozonolysis of  $\alpha$ -pinene disproportional to its concentration. However, additional  
328 field measurements should be performed in order to estimate the contribution of these compounds to  
329 aerosol particles. Because amines are ubiquitous in the atmosphere,<sup>6</sup> similar reactions in ambient  
330 conditions could be important for the formation and growth of SOAs in the atmosphere. Finally, more  
331 laboratory studies are needed to elucidate the formation pathways and quantify the impact of amine  
332 reactions on the SOA formation.

## 333 ASSOCIATED CONTENT

### 334 **Supporting Information.**

335 Figure S1 presents the scheme of the experimental set-up used in this work. Figure S2 shows the  
336 representative high-resolution mass spectra obtained by HR-ToF-CIMS from the laboratory  
337 experiments. Figure S3 presents the mass defect plot of reaction products identified by HR-ToF-  
338 CIMS from the ozonolysis of  $\alpha$ -pinene in presence and absence of DMA. Figures S4-S7 describe the  
339 results from quantum chemistry calculations. Figure S8 displays the proposed mechanism for the  
340 formation of  $C_9H_{14}O_2$ ,  $C_9H_{14}O_3$  and  $C_3H_7O_2N$  from the ozonolysis of enamine arising from the  
341 pinonaldehyde-DMA reaction. Figure S9 presents the  $MS^2$  fragmentation patterns of selected product  
342 ions, leading to the formation of a fragment ion at  $m/z$  72.044. Figure S10 gives a proposed  
343 mechanism for tertiary amide reaction products obtained from organic acids-DMA reactions. Figure  
344 S11 presents the  $MS^2$  fragmentation pathway of the product ion at  $m/z$  198.149. Figure S12 shows  
345 the  $MS^2$  fragmentation pattern of product ions at  $m/z$  198.149 and 212.164 from laboratory and field  
346 samples. Figure S13 presents the concentration in  $ng.m^{-3}$  of reaction products identified in Hyytiälä,



347 Finland. Table S1 lists the N-containing compounds detected by HR-ToF-CIMS from the ozonolysis  
348 of  $\alpha$ -pinene in the presence of DMA. Table S2 presents the Gibbs free energies relative to the reactants  
349 at 298.15K. This material is available free of charge via the Internet at <http://pubs.acs.org>.

## 350 AUTHOR INFORMATION

### 351 Corresponding Author

352 \*Marja-Liisa Riekkola. Tel: +358 405058848. E-mail address: [marja-liisa.riekkola@helsinki.fi](mailto:marja-liisa.riekkola@helsinki.fi)

### 353 Notes

354 The authors declare no competing financial interest.

355

## 356 ACKNOWLEDGMENT

357 The financial support of the Academy of Finland Center of Excellence program (project no 272041),  
358 European Research Council (COALA, grant 638703 and MOCAPAF, grant 57360) is gratefully  
359 acknowledged. The CSC-IT Center for Science in Espoo (Finland) is also thank for computational  
360 resources. Technical staff at the SMEAR II Station are thanked for the valuable help. SPME Arrows  
361 were kindly provided by CTC Analytik (Switzerland).

## 362 REFERENCE

- 363 1. Pope III, C. A.; Dockery, D. W. Health effects of fine particulate air pollution: lines that connect. *J. Air Waste*  
364 *Manage. Assoc.* **2006**, 56 (6), 709–742.
- 365 2. IPCC, Climate Change 2013: The Physical Science Basis: Working Group I Contribution to the Fifth  
366 Assessment Report of the Intergovernmental Panel on Climate Change. Cambridge University Press: 2013.
- 367 3. Kanakidou, M.; Seinfeld, J.; Pandis, S.; Barnes, I.; Dentener, F.; Facchini, M.; Dingenen, R. V.; Ervens, B.;  
368 Nenes, A.; Nielsen, C. Organic aerosol and global climate modelling: a review. *Atmos. Chem. Phys.* **2005**, 5  
369 (4), 1053–1123.
- 370 4. Hallquist, M.; Wenger, J.; Baltensperger, U.; Rudich, Y.; Simpson, D.; Claeys, M.; Dommen, J.; Donahue, N.;  
371 George, C.; Goldstein, A. H.; Hamilton, J. F.; Herrmann, H.; Hoffmann, T.; Iinuma, Y.; Jang, M.; Jenkin, M. E.;

- 372 Jimenez, J. L.; Kiendler-Scharr, A.; Maenhaut, W.; McFiggans, G.; Mentel, Th. F.; Monod, A.; Prévôt, A. S. H.;  
373 Seinfeld, J. H.; Surratt, J. D.; Szmigielski, R.; Wildt, J. The formation, properties and impact of secondary  
374 organic aerosol: current and emerging issues. *Atmos. Chem. Phys.* **2009**, *9* (14), 5155–5236.
- 375 5. Ziemann, P. J.; Atkinson, R. Kinetics, products, and mechanisms of secondary organic aerosol formation.  
376 *Chem. Soc. Rev.* **2012**, *41* (19), 6582–6605.
- 377 6. Ge, X.; Wexler, A. S.; Clegg, S. L. Atmospheric amines—Part I. A review. *Atmos. Environ.* **2011**, *45* (3),  
378 524–546.
- 379 7. Kieloaho, A.-J.; Hellén, H.; Hakola, H.; Manninen, H. E.; Nieminen, T.; Kulmala, M.; Pihlatie, M. Gas-phase  
380 alkylamines in a boreal Scots pine forest air. *Atmos. Environ.* **2013**, *80*, 369–377.
- 381 8. Youn, J.-S.; Crosbie, E.; Maudlin, L.; Wang, Z.; Sorooshian, A., Dimethylamine as a major alkyl amine species  
382 in particles and cloud water: Observations in semi-arid and coastal regions. *Atmos. Environ.* **2015**, *122*,  
383 250–258.
- 384 9. Almeida, J.; Schobesberger, S.; Kuerten, A.; Ortega, I. K.; Kupiainen-Maatta, O.; Praplan, A. P.; Adamov, A.;  
385 Amorim, A.; Bianchi, F.; Breitenlechner, M.; David, A.; Dommen, J.; Donahue, N. M.; Downard, A.; Dunne, E.;  
386 Duplissy, J.; Ehrhart, S.; Flagan, R. C.; Franchin, A.; Guida, R.; Hakala, J.; Hansel, A.; Heinritzi, M.; Henschel, H.;  
387 Jokinen, T.; Junninen, H.; Kajos, M.; Kangasluoma, J.; Keskinen, H.; Kupc, A.; Kurten, T.; Kvashin, A. N.;  
388 Laaksonen, A.; Lehtipalo, K.; Leiminger, M.; Leppä, J.; Loukonen, V.; Makhmutov, V.; Mathot, S.; McGrath, M.  
389 J.; Nieminen, T.; Olenius, T.; Onnela, A.; Petaja, T.; Riccobono, F.; Riipinen, I.; Rissanen, M.; Rondo, L.;  
390 Ruuskanen, T.; Santos, F. D.; Sarnela, N.; Schallhart, S.; Schnitzhofer, R.; Seinfeld, J. H.; Simon, M.; Sipila, M.;  
391 Stozhkov, Y.; Stratmann, F.; Tome, A.; Troestl, J.; Tsagkogeorgas, G.; Vaattovaara, P.; Viisanen, Y.; Virtanen,  
392 A.; Vrtala, A.; Wagner, P. E.; Weingartner, E.; Wex, H.; Williamson, C.; Wimmer, D.; Ye, P.; Yli-Juuti, T.; Carslaw,  
393 K. S.; Kulmala, M.; Curtius, J.; Baltensperger, U.; Worsnop, D. R.; Vehkamäki, H.; Kirkby, J. Molecular  
394 understanding of sulphuric acid-amine particle nucleation in the atmosphere. *Nature* **2013**, *502* (7471),  
395 359–363.
- 396 10. Yu, H.; McGraw, R.; Lee, S. H. Effects of amines on formation of sub-3 nm particles and their subsequent  
397 growth. *Geophys. Res. Lett.* **2012**, *39* (2), L02807.
- 398 11. Qiu, C.; Zhang, R., Multiphase chemistry of atmospheric amines. *Phys. Chem. Chem. Phys.* **2013**, *15* (16),  
399 5738–5752.
- 400 12. Tao, Y.; Ye, X.; Jiang, S.; Yang, X.; Chen, J.; Xie, Y.; Wang, R. Effects of amines on particle growth observed  
401 in new particle formation events. *Journal of Geophysical Research: Atmospheres* **2016**, *121* (1), 324–335.
- 402 13. Glasoe, W.; Volz, K.; Panta, B.; Freshour, N.; Bachman, R.; Hanson, D.; McMurry, P.; Jen, C. Sulfuric acid  
403 nucleation: An experimental study of the effect of seven bases. *Journal of Geophysical Research:*  
404 *Atmospheres* **2015**, *120* (5), 1933–1950.
- 405 14. Kurtén, T.; Loukonen, V.; Vehkamäki, H.; Kulmala, M. Amines are likely to enhance neutral and ion-  
406 induced sulfuric acid-water nucleation in the atmosphere more effectively than ammonia. *Atmos. Chem.*  
407 *Phys.* **2008**, *8* (14), 4095–4103.
- 408 15. Erupe, M.; Viggiano, A.; Lee, S.-H. The effect of trimethylamine on atmospheric nucleation involving  
409 H<sub>2</sub>SO<sub>4</sub>. *Atmos. Chem. Phys.* **2011**, *11* (10), 4767–4775.
- 410 16. Kurten, A.; Jokinen, T.; Simon, M.; Sipila, M.; Sarnela, N.; Junninen, H.; Adamov, A.; Joao Almeida, A.;  
411 Amorim, A.; Bianchi, F.; Breitenlechner, M.; Dommen, J.; Donahue, N. M.; Duplissy, J.; Ehrhart, S.; Flagan, R.  
412 C.; Franchin, A.; Hakala, J.; Hansel, A.; Heinritzi, M.; Hutterli, M.; Kangasluoma, J.; Kirkby, J.; Laaksonen, A.;

413 Lehtipalo, K.; Leiminger, M.; Makhmutov, V.; Mathot, S.; Onnela, A.; Petaja, T.; Praplan, A. P.; Riccobono, F.;  
 414 Rissanen, M. P.; Rondo, L.; Schobesberger, S.; Seinfeld, J. H.; Steiner, G.; Tome, A.; Trostl, J.; Winkler, P. M.;  
 415 Williamson, C.; Wimmer, D.; Ye, P.; Baltensperger, U.; Carslaw, K. S.; Kulmala, M.; Worsnop, D. R.; Curtius, J.  
 416 Neutral molecular cluster formation of sulfuric acid–dimethylamine observed in real time under atmospheric  
 417 conditions. *Proc. Natl. Acad. Sci. USA* **2014**, *111* (42), 15019–15024.

418 17. Mäkelä, J.; Yli-Koivisto, S.; Hiltunen, V.; Seidl, W.; Swietlicki, E.; Teinilä, K.; Sillanpää, M.; Koponen, I.;  
 419 Paatero, J.; Rosman, K. Chemical composition of aerosol during particle formation events in boreal forest.  
 420 *Tellus B* **2001**, *53* (4), 380–393.

421 18. Smith, J. N.; Barsanti, K. C.; Friedli, H. R.; Ehn, M.; Kulmala, M.; Collins, D. R.; Scheckman, J. H.; Williams,  
 422 B. J.; McMurry, P. H., Observations of aminium salts in atmospheric nanoparticles and possible climatic  
 423 implications. *Proc. Natl. Acad. Sci. USA* **2010**, *107* (15), 6634–6639.

424 19. Zhao, J.; Smith, J.; Eisele, F.; Chen, M.; Kuang, C.; McMurry, P. Observation of neutral sulfuric acid-amine  
 425 containing clusters in laboratory and ambient measurements. *Atmos. Chem. Phys.* **2011**, *11* (21),  
 426 10823–10836.

427 20. Galloway, M. M.; Powelson, M. H.; Sedehi, N.; Wood, S. E.; Millage, K. D.; Kononenko, J. A.; Rynaski, A. D.;  
 428 De Haan, D. O. Secondary organic aerosol formation during evaporation of droplets containing atmospheric  
 429 aldehydes, amines, and ammonium sulfate. *Environ. Sci. Technol.* **2014**, *48* (24), 14417–14425.

430 21. De Haan, D. O.; Hawkins, L. N.; Kononenko, J. A.; Turley, J. J.; Corrigan, A. L.; Tolbert, M. A.; Jimenez, J. L.  
 431 Formation of nitrogen-containing oligomers by methylglyoxal and amines in simulated evaporating cloud  
 432 droplets. *Environ. Sci. Technol.* **2010**, *45* (3), 984–991.

433 22. Duporté, G.; Parshintsev, J.; Barreira, L. s. M.; Hartonen, K.; Kulmala, M.; Riekkola, M.-L. Nitrogen-  
 434 Containing Low Volatile Compounds from Pinonaldehyde-Dimethylamine Reaction in the Atmosphere: A  
 435 Laboratory and Field Study. *Environ. Sci. Technol.* **2016**, *50* (9), 4693–4700.

436 23. Stropoli, S. J.; Elrod, M. J. Assessing the Potential for the Reactions of Epoxides with Amines on Secondary  
 437 Organic Aerosol Particles. *J. Phys. Chem. A* **2015**, *119* (40), 10181–10189.

438 24. Lavi, A.; Segre, E.; Gomez-Hernandez, M.; Zhang, R.; Rudich, Y. Volatility of atmospherically relevant  
 439 alkylaminium carboxylate. *J. Phys. Chem. A* **2015**, *119* (19), 4336–4346.

440 25. Gomez-Hernandez, M.; McKeown, M.; Secrest, J.; Marrero-Ortiz, W.; Lavi, A.; Rudich, Y.; Collins, D. R.;  
 441 Zhang, R. Hygroscopic characteristics of alkylaminium carboxylate aerosols. *Environ. Sci. Technol.* **2016**, *50* (5),  
 442 2292–2300.

443 26. Rissanen, M. P.; Kurtén, T.; Sipilä, M.; Thornton, J. A.; Kangasluoma, J.; Sarnela, N.; Junninen, H.;  
 444 Jørgensen, S.; Schallhart, S.; Kajos, M. K.; Taipale, R.; Springer, M.; Mentel, T. G.; Petäjä, T.; Worsnop, D. R.;  
 445 Kjaergaard, H. G.; Ehn, M. The formation of highly oxidized multifunctional products in the ozonolysis of  
 446 cyclohexene. *J. Am. Chem. Soc.* **2014**, *136* (44), 15596–15606.

447 27. Rissanen, M. P.; Kurtén, T.; Sipilä, M.; Thornton, J. A.; Kausiala, O.; Garmash, O.; Kjaergaard, H. G.; Petäjä,  
 448 T.; Worsnop, D. R.; Ehn, M. Effects of chemical complexity on the autoxidation mechanisms of endocyclic  
 449 alkene ozonolysis products: From methylcyclohexenes toward understanding  $\alpha$ -pinene. *J. Phys. Chem. A*  
 450 **2015**, *119* (19), 4633–4650.

451 28. Hawkins, J. E.; Armstrong, G. T. Physical and Thermodynamic Properties of Terpenes. 1 III. The Vapor  
 452 Pressures of  $\alpha$ -Pinene and  $\beta$ -Pinene. *J. Am. Chem. Soc.* **1954**, *76* (14), 3756–3758.

- 453 29. Helin, A.; Rönkkö, T.; Parshintsev, J.; Hartonen, K.; Schilling, B.; Läubli, T.; Riekkola, M.-L. Solid phase  
454 microextraction Arrow for the sampling of volatile amines in wastewater and atmosphere. *J. Chromatogr. A*  
455 **2015**, 1426, 56–63.
- 456 30. Lee, B. H.; Lopez-Hilfiker, F. D.; Mohr, C.; Kurtén, T.; Worsnop, D. R.; Thornton, J. A. An iodide-adduct  
457 high-resolution time-of-flight chemical-ionization mass spectrometer: Application to atmospheric inorganic  
458 and organic compounds. *Environ. Sci. Technol.* **2014**, 48 (11), 6309–6317.
- 459 31. Lopez-Hilfiker, F. D.; Lee, B. H.; D'Ambro, E. L.; Thornton, J. A. Constraining the sensitivity of iodide adduct  
460 chemical ionization mass spectrometry to multifunctional organic molecules using the collision limit and  
461 thermodynamic stability of iodide ion adducts. *Atmos. Meas. Tech.* **2016**, 9 (4), 1505–1512.
- 462 32. Lopez-Hilfiker, F.; Mohr, C.; D'Ambro, E. L.; Lutz, A.; Riedel, T. P.; Gaston, C. J.; Iyer, S.; Zhang, Z.; Gold, A.;  
463 Surratt, J. D.; Lee, B. H.; Kurten, T.; Hu, W. W.; Jimenez, J.; Hallquist, M.; Thornton, J. A. Molecular  
464 Composition and Volatility of Organic Aerosol in the Southeastern US: Implications for IEPOX Derived SOA.  
465 *Environ. Sci. Technol.* **2016**, 50 (5), 2200–2209.
- 466 33. Hari, P.; Kulmala, M. Station for measuring ecosystem-atmosphere relations. *Boreal Environ. Res.* **2005**,  
467 10 (5), 315–322.
- 468 34. Rinne, J.; Hakola, H.; Laurila, T.; Rannik, Ü. Canopy scale monoterpene emissions of *Pinus sylvestris*  
469 dominated forests. *Atmos. Environ.* **2000**, 34 (7), 1099–1107.
- 470 35. Berndt, T.; Sipilä, M.; Stratmann, F.; Petäjä, T.; Vanhanen, J.; Mikkilä, J.; Patokoski, J.; Taipale, R.; Mauldin  
471 III, R. L.; Kulmala, M. Enhancement of atmospheric H<sub>2</sub>SO<sub>4</sub>/H<sub>2</sub>O nucleation: organic oxidation products versus  
472 amines. *Atmos. Chem. Phys.* **2014**, 14 (2), 751–764.
- 473 36. Berndt, T.; Stratmann, F.; Sipilä, M.; Vanhanen, J.; Petäjä, T.; Mikkilä, J.; Grüner, A.; Spindler, G.; Mauldin  
474 III, L.; Curtius, J.; Kulmala, M.; Heintzenberg, J. Laboratory study on new particle formation from the reaction  
475 OH + SO<sub>2</sub>: influence of experimental conditions, H<sub>2</sub>O vapour, NH<sub>3</sub> and the amine tert-butylamine on the  
476 overall process. *Atmos. Chem. Phys.* **2010**, 10 (15), 7101–7116.
- 477 37. Zollner, J.; Glasoe, W.; Panta, B.; Carlson, K.; McMurry, P.; Hanson, D. Sulfuric acid nucleation: power  
478 dependencies, variation with relative humidity, and effect of bases. *Atmos. Chem. Phys.* **2012**, 12 (10),  
479 4399–4411.
- 480 38. Xu, W.; Zhang, R. A theoretical study of hydrated molecular clusters of amines and dicarboxylic acids. *J.*  
481 *Chem. Phys.* **2013**, 139 (6), 064312.
- 482 39. Ehn, M.; Thornton, J. A.; Kleist, E.; Sipilä, M.; Junninen, H.; Pullinen, I.; Springer, M.; Rubach, F.; Tillmann,  
483 R.; Lee, B.; Lopez-Hilfiker, F.; Andres, S.; Acir, I.-H.; Rissanen, M.; Jokinen, T.; Schobesberger, S.; Kangasluoma,  
484 J.; Kontkanen, J.; Nieminen, T.; Kurten, T.; Nielsen, L. B.; Jorgensen, S.; Kjaergaard, H. G.; Canagaratna, M.;  
485 Maso, M. D.; Berndt, T.; Petaja, T.; Wahner, A.; Kerminen, V.-M.; Kulmala, M.; Worsnop, D. R.; Wildt, J.;  
486 Mentel, T. F. A large source of low-volatility secondary organic aerosol. *Nature* **2014**, 506 (7489), 476–479.
- 487 40. Mutzel, A.; Poulain, L.; Berndt, T.; Iinuma, Y.; Rodigast, M.; Böge, O.; Richters, S.; Spindler, G.; Sipilä, M.;  
488 Jokinen, T.; Kulmala, M.; Herrmann, H. Highly oxidized multifunctional organic compounds observed in  
489 tropospheric particles: A field and laboratory study. *Environ. Sci. Technol.* **2015**, 49 (13), 7754–7761.
- 490 41. Tu, P.; Hall IV, W. A.; Johnston, M. V. Characterization of Highly Oxidized Molecules in Fresh and Aged  
491 Biogenic Secondary Organic Aerosol. *Anal. Chem.* **2016**, 88 (8), 4495–4501.

- 492 42. Kendrick, E. A Mass Scale Based on  $\text{CH}_2 = 14.0000$  for High Resolution Mass Spectrometry of Organic  
493 Compounds. *Anal. Chem.* **1963**, 35 (13), 2146–2154.
- 494 43. Walser, M. L.; Desyaterik, Y.; Laskin, J.; Laskin, A.; Nizkorodov, S. A. High-resolution mass spectrometric  
495 analysis of secondary organic aerosol produced by ozonation of limonene. *Phys. Chem. Chem. Phys.* **2008**, 10  
496 (7), 1009–1022.
- 497 44. Jang, M.; Kamens, R. M. Newly characterized products and composition of secondary aerosols from the  
498 reaction of  $\alpha$ -pinene with ozone. *Atmos. Environ.* **1999**, 33 (3), 459–474.
- 499 45. Gomez, S.; Peters, J. A.; Maschmeyer, T. The reductive amination of aldehydes and ketones and the  
500 hydrogenation of nitriles: mechanistic aspects and selectivity control. *Adv. Synth. Catal.* **2002**, 344 (10),  
501 1037–1058.
- 502 46. Zahardis, J.; Geddes, S.; Petrucci, G. The ozonolysis of primary aliphatic amines in fine particles. *Atmos.*  
503 *Chem. Phys.* **2008**, 8 (5), 1181–1194.
- 504 47. Sareen, N.; Waxman, E. M.; Turpin, B. J.; Volkamer, R.; Carlton A. G. Potential of aerosol liquid water to  
505 facilitate organic aerosol formation: assessing knowledge gaps about precursors and partitioning. *Environ.*  
506 *Sci. Technol.* **2017**, 51 (6), 3327–3335.
- 507 48. Onel, L.; Thonger, L.; Blitz, M.; Seakins, P.; Bunkan, A.; Solimannejad, M.; Nielsen, C. Gas-Phase Reactions  
508 of OH with Methyl Amines in the Presence or Absence of Molecular Oxygen. An Experimental and Theoretical  
509 Study. *J. Phys. Chem. A* **2013**, 117 (41), 10736–10745.
- 510 49. Tuazon, E. C.; Atkinson, R.; Aschmann, S. M.; Arey, J. Kinetics and products of the gas-phase reactions of  
511  $\text{O}_3$  with amines and related compounds. *Res. Chem. Intermed.* **1994**, 20 (3-5), 303–320.
- 512 50. De Haan, D. O.; Tolbert, M. A.; Jimenez, J. L. Atmospheric condensed-phase reactions of glyoxal with  
513 methylamine. *Geophys. Res. Lett.* **2009**, 36 (11), L11819.
- 514 51. Jenkin, M. E.; Shallcross, D. E.; Harvey, J. N. Development and application of a possible mechanism for the  
515 generation of cis-pinic acid from the ozonolysis of  $\alpha$ - and  $\beta$ -pinene. *Atmos. Environ.* **2000**, 34 (18), 2837–2850.
- 516 52. Ge, Y.; Liu, Y.; Chu, B.; He, H.; Chen, T.; Wang, S.; Wei, W.; Cheng, S. Ozonolysis of Trimethylamine  
517 Exchanged with Typical Ammonium Salts in the Particle Phase. *Environ. Sci. Technol.* **2016**, 50 (20),  
518 11076–11084.
- 519 53. Barsanti, K. C.; Pankow, J. F. Thermodynamics of the formation of atmospheric organic particulate matter  
520 by accretion reactions—Part 3: Carboxylic and dicarboxylic acids. *Atmos. Environ.* **2006**, 40 (34), 6676–6686.
- 521 54. Surratt, J. D.; Gómez-González, Y.; Chan, A. W.; Vermeylen, R.; Shahgholi, M.; Kleindienst, T. E.; Edney, E.  
522 O.; Offenberg, J. H.; Lewandowski, M.; Jaoui, M.; Maenhaut, W.; Claeys, M.; Flagan, R. C.; Seinfeld, J. H.,  
523 Organosulfate formation in biogenic secondary organic aerosol. *J. Phys. Chem. A* **2008**, 112 (36), 8345–8378.
- 524 55. Anttila, P.; Rissanen, T.; Shimmo, M.; Kallio, M.; Hyötyläinen, T.; Kulmala, M.; Riekkola, M.-L. Organic  
525 compounds in atmospheric aerosols from a Finnish coniferous forest. *Boreal Environ. Res.* **2005**, 10 (5),  
526 371–384.
- 527 56. Jaoui, M.; Kamens, R. M. Mass balance of gaseous and particulate products analysis from  $\alpha$ -pinene/ $\text{NO}_x$ /air in the presence of natural sunlight. *J. Geophys. Res. Atmos.* **2001**, 106 (D12), 12541–12558.

529 57. Kristensen, K.; Enggrob, K. L.; King, S. M.; Worton, D.; Platt, S.; Mortensen, R.; Rosenoern, T.; Surratt, J.;  
 530 Bilde, M.; Goldstein, A.; Glasius, M., Formation and occurrence of dimer esters of pinene oxidation products  
 531 in atmospheric aerosols. *Atmos. Chem. Phys.* **2013**, *13* (7), 3763–3776.

532 58. Kristensen, K.; Cui, T.; Zhang, H.; Gold, A.; Glasius, M.; Surratt, J. D. Dimers in  $\alpha$ -pinene secondary organic  
 533 aerosol: effect of hydroxyl radical, ozone, relative humidity and aerosol acidity. *Atmos. Chem. Phys.* **2014**, *14*  
 534 (8), 4201–4218.

536

537

538 **Table 1.** Summary of the Experimental Conditions

| Experiments | Initial<br>[ $\alpha$ -pinene]<br>(ppm) | Initial<br>[O <sub>3</sub> ]<br>(ppb) | Initial<br>[DMA]<br>(ppb) | Residence<br>time (s) | Final<br>[O <sub>3</sub> ]<br>(ppb) | Number of<br>particles<br>- <sup>3</sup><br>(#.cm <sup>-3</sup> ) |
|-------------|---|---------------------------------------|---------------------------|-----------------------|-------------------------------------|---|
| E1          | 5.0                                     | 104.4                                 | -                         | 53                    | 38.5                                | 25800 ± 4500  |
| E1'         | 5.0                                     | 104.4                                 | 500                       | 53                    | 8.8                                 | 76300 ± 3100  |
| E2          | 5.0                                     | 113.0                                 | -                         | 53                    | 42.9                                | 9500 ± 2000   |
| E2'         | 5.0                                     | 113.0                                 | 500                       | 53                    | 7.5                                 | 71300 ± 3200  |
| E3          | 5.0                                     | 116.4                                 | -                         | 53                    | 43.5                                | 15500 ± 2500  |
| E3'         | 5.0                                     | 116.4                                 | 500                       | 53                    | 8.2                                 | 71700 ± 1500  |
| E4          | 7.0                                     | 130.0                                 | 700                       | 56                    | 3.1                                 | 93300 ± 2500  |

539

540

**Table 2.** N-containing compounds detected in filter and flow tube wall samples by UHPLC-HRMS in positive mode from  $\alpha$ -pinene-O<sub>3</sub>-DMA experiment.  $\Delta m$  is the difference in ppm between theoretical masses and experimental masses of the ions.

| [M+H] <sup>+</sup><br>detected<br>ions<br>(m/z) | molecular<br>formula  | $\Delta m$<br>(ppm) | % of the total<br>N-containing<br>compounds<br>identified in<br>particulate<br>phase <sup>a</sup> | Tertiary<br>amide<br>functionality<br>MS <sup>2</sup> fragment<br>C <sub>3</sub> H <sub>6</sub> ON <sup>+</sup><br>(m/z 72.0444) | Detected in gas<br>phase  |                                    | Detected<br>in PM <sub>1</sub><br>ambient<br>samples |
|---|---|---------------------|---|--|---------------------------|------------------------------------|--|
|   |   |                     |   |  | HR-<br>CI-<br>APi-<br>TOF | SPE<br>cartridge<br>UHPLC-<br>HRMS |  |
| 176.09171                                       | C <sub>7</sub> H <sub>13</sub> O <sub>4</sub> N               | - 0.26              | < 1 <sup>b</sup>  | X  | X                         |                                    |  |
| 186.11244                                       | C <sub>9</sub> H <sub>15</sub> O <sub>3</sub> N               | 0.01                | < 1 <sup>b</sup>  | X  | X                         |                                    |  |
| 196.13366                                       | C <sub>11</sub> H <sub>17</sub> O <sub>2</sub> N              | - 0.04              | < 1 <sup>b</sup>  | X  |                           | X                                  | X <sup>f</sup>                                       |
| 196.16959                                       | C <sub>12</sub> H <sub>21</sub> ON                            | - 0.01              | < 1 <sup>b</sup>  |  |                           | X                                  | X <sup>f,g</sup>                                     |
| 198.14880                                       | C <sub>11</sub> H <sub>19</sub> O <sub>2</sub> N              | - 0.26              | 7 ± 3 <sup>b</sup>  | X  | X                         | X                                  | X <sup>e</sup>                                       |
| 200.12796                                       | C <sub>10</sub> H <sub>17</sub> O <sub>3</sub> N              | - 0.79              | 6 ± 3 <sup>b</sup>  | X  | X                         | X                                  | X <sup>f</sup>                                       |
| 208.10800                                       | C <sub>10</sub> H <sub>13</sub> O <sub>2</sub> N <sub>3</sub> | -0.24               | 2 ± 3 <sup>c</sup>  |  |                           |                                    |  |
| 210.14890                                       | C <sub>12</sub> H <sub>19</sub> O <sub>2</sub> N              | - 0.21              | < 1 <sup>b</sup>  | X  | X                         | X                                  |  |
| 212.16443                                       | C <sub>12</sub> H <sub>21</sub> O <sub>2</sub> N              | - 0.36              | 35 ± 2 <sup>b</sup>   | X  | X                         | X                                  | X <sup>e</sup>                                       |
| 214.14368                                       | C <sub>11</sub> H <sub>19</sub> O <sub>3</sub> N              | - 0.38              | < 1 <sup>b</sup>  | X  | X                         |                                    |  |
| 216.12294                                       | C <sub>10</sub> H <sub>17</sub> O <sub>4</sub> N              | - 0.45              | < 1 <sup>b</sup>  |  | X                         |                                    |  |
| 226.14366                                       | C <sub>12</sub> H <sub>19</sub> O <sub>3</sub> N              | - 0.65              | 26 ± 15 <sup>b</sup>  | X  | X                         | X                                  |  |
| 228.15930                                       | C <sub>12</sub> H <sub>21</sub> O <sub>3</sub> N              | - 0.38              | 3 ± 1 <sup>b</sup>  | X  | X                         | X                                  |  |
| 230.13858                                       | C <sub>11</sub> H <sub>19</sub> O <sub>4</sub> N              | - 0.38              | < 1 <sup>b</sup>  | X  | X                         |                                    |  |
| 241.19099                                       | C <sub>13</sub> H <sub>24</sub> O <sub>2</sub> N <sub>2</sub> | - 0.23              | - <sup>d</sup>  |  |                           |                                    |  |
| 244.15422                                       | C <sub>12</sub> H <sub>21</sub> O <sub>4</sub> N              | - 0.46              | < 1 <sup>b</sup>  |  |                           |                                    |  |
| 266.11325                                       | C <sub>12</sub> H <sub>15</sub> O <sub>4</sub> N <sub>3</sub> | 1.07                | < 1 <sup>c</sup>  |  |                           |                                    |  |
| 280.12920                                       | C <sub>13</sub> H <sub>17</sub> O <sub>4</sub> N <sub>3</sub> | - 0.42              | 15 ± 14 <sup>c</sup>  |  |                           |                                    |  |
| 300.15506                                       | C <sub>13</sub> H <sub>21</sub> O <sub>5</sub> N <sub>3</sub> | 1.13                | < 1 <sup>c</sup>  |  |                           |                                    |  |
| 308.16010                                       | C <sub>15</sub> H <sub>21</sub> O <sub>4</sub> N <sub>3</sub> | 1.20                | < 1 <sup>b</sup>  |  |                           |                                    |  |
| 334.22200                                       | C <sub>16</sub> H <sub>31</sub> O <sub>6</sub> N              | - 0.54              | - <sup>d</sup>  |  |                           |                                    |  |
| 342.22729                                       | C <sub>18</sub> H <sub>31</sub> O <sub>5</sub> N              | - 0.54              | < 1 <sup>b</sup>  |  |                           |                                    |  |
| 358.25861                                       | C <sub>19</sub> H <sub>35</sub> O <sub>5</sub> N              | - 0.62              | - <sup>d</sup>  |  |                           |                                    |  |
| 364.16119                                       | C <sub>16</sub> H <sub>21</sub> O <sub>5</sub> N <sub>5</sub> | 0.98                | < 1 <sup>b</sup>  |  |                           |                                    |  |
| 364.26923                                       | C <sub>18</sub> H <sub>37</sub> O <sub>6</sub> N              | - 0.54              | - <sup>d</sup>  |  |                           |                                    |  |
| 376.19638                                       | C <sub>17</sub> H <sub>29</sub> O <sub>8</sub> N              | - 0.48              | - <sup>d</sup>  |  |                           |                                    |  |
| 384.17606                                       | C <sub>17</sub> H <sub>25</sub> O <sub>7</sub> N <sub>3</sub> | 1.22                | < 1 <sup>c</sup>  |  |                           |                                    |  |
| 388.19678                                       | C <sub>18</sub> H <sub>29</sub> O <sub>8</sub> N              | - 0.62              | - <sup>d</sup>  |  |                           |                                    |  |
| 390.28491                                       | C <sub>20</sub> H <sub>39</sub> O <sub>6</sub> N              | - 0.34              | - <sup>d</sup>  |  |                           |                                    |  |
| 394.31610                                       | C <sub>20</sub> H <sub>43</sub> O <sub>6</sub> N              | - 0.61              | - <sup>d</sup>  |  |                           |                                    |  |
| 401.13489                                       | C <sub>20</sub> H <sub>20</sub> O <sub>7</sub> N <sub>2</sub> | -1.01               | < 1 <sup>b</sup>  |  |                           |                                    |  |
| 411.17007                                       | C <sub>26</sub> H <sub>22</sub> O <sub>3</sub> N <sub>2</sub> | 0.61                | < 1 <sup>b</sup>  |  |                           |                                    |  |
| 442.21826                                       | C <sub>20</sub> H <sub>31</sub> O <sub>8</sub> N <sub>3</sub> | 0.3                 | < 1 <sup>b</sup>  |  |                           |                                    |  |
| 444.33182                                       | C <sub>24</sub> H <sub>45</sub> O <sub>6</sub> N              | - 0.11              | - <sup>d</sup>  |  |                           |                                    |  |
| 488.35812                                       | C <sub>26</sub> H <sub>45</sub> O <sub>6</sub> N              | 0.15                | - <sup>d</sup>  |  |                           |                                    |  |
| 504.20868                                       | C <sub>23</sub> H <sub>29</sub> O <sub>8</sub> N <sub>5</sub> | 0.42                | < 1 <sup>c</sup>  |  |                           |                                    |  |
| 532.38452                                       | C <sub>28</sub> H <sub>53</sub> O <sub>8</sub> N              | - 0.09              | - <sup>d</sup>  |  |                           |                                    |  |
| 576.41060                                       | C <sub>30</sub> H <sub>57</sub> O <sub>9</sub> N              | - 0.01              | - <sup>d</sup>  |  |                           |                                    |  |

<sup>a</sup>Peak area (ion<sub>i</sub>)/ΣPeak area (ions)

<sup>b</sup>detected in aerosol samples and in the flow tube wall samples

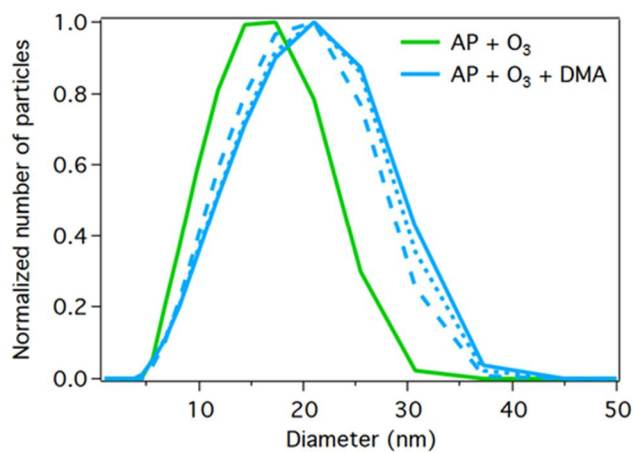
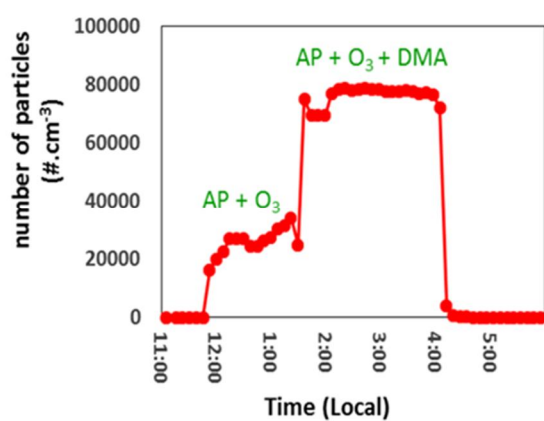
<sup>c</sup>only detected in aerosol samples

<sup>d</sup>only detected in the flow tube wall samples

<sup>e</sup>confirmed by retention times, accurate masses and MS-MS fragmentation patterns

<sup>f</sup>confirmed by accurate masses

<sup>g</sup>previously observed in ambient samples<sup>22</sup>



551

552 **Figure 1.** Particle number concentration (left) and particle size distribution (right) from  $\alpha$ -pinene- $O_3$   
 553 experiment (E1) and  $\alpha$ -pinene- $O_3$ -DMA experiment (E1'). The blue curves represent 3 different times of the  
 554 particle size distribution from  $\alpha$ -pinene- $O_3$ -DMA experiment.

555



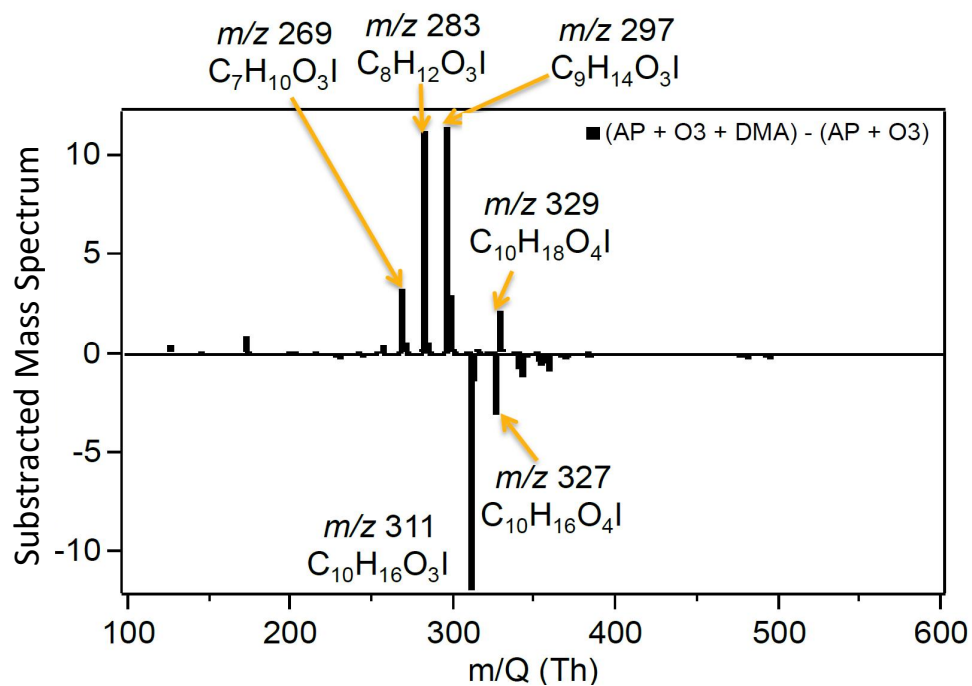


**Figure 2.** Difference in Mass Spectra from  $\alpha$ -pinene- $O_3$ -DMA (experiment E2') and  $\alpha$ -pinene- $O_3$  experiments (experiment E2). Positive signals correspond to new products formed in the presence of DMA and negative signals are compounds lost when DMA is introduced.

567

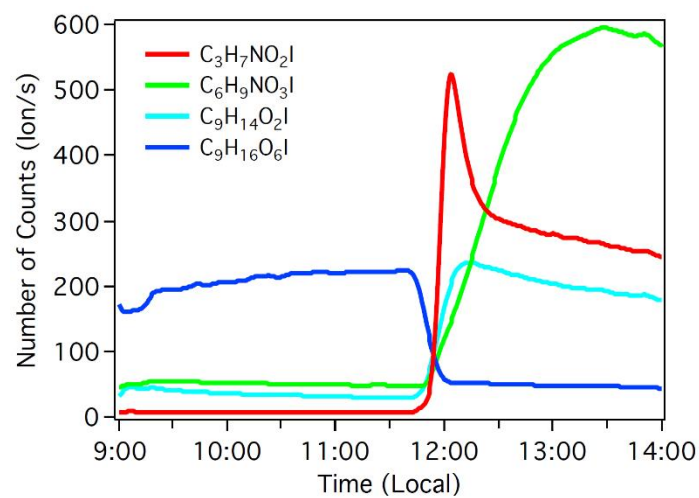
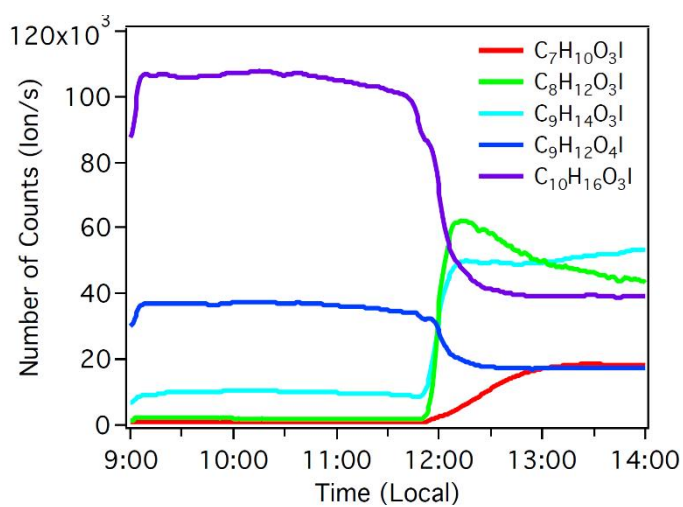
568

569

570

571

572



573

574

575

576

**Figure 3.** Temporal profiles of selected ion HR-ToF-CIMS (Experiments E2 and E2'), DMA was injected at 11:45.  $C_9H_{14}O_4I$  ion is attributed to nor-pinonic acid signal,  $C_{10}H_{16}O_3I$  to pinonic acid signal, and  $C_9H_{14}O_2I$  to nor-pinonaldehyde signal.

577  
578  
579  
580  
581  
582  
583  
584  
585  
586  
587  
588  
589  
590  
591  
592  
593  
594  
595  
596  
597  
598  
599  
600  
601  
602

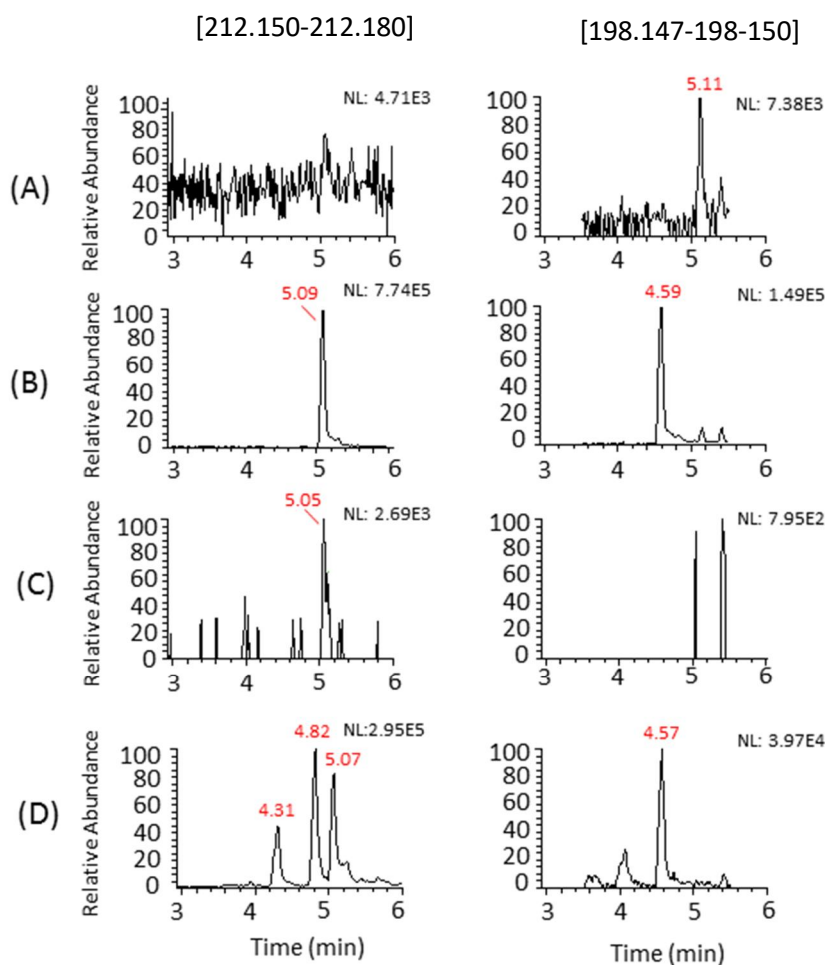


**Figure 4.** Extracted ion chromatograms of  $m/z$  198.1489  $\pm$  0.0015 and 212.1644  $\pm$  0.0015 from (A)  $\alpha$ -pinene + O<sub>3</sub> experiment, (B)  $\alpha$ -pinene + O<sub>3</sub> + DMA experiment, (C) blank filter sample, and (D) PM<sub>1</sub> sample collected in Hyytiälä (23<sup>th</sup> of May, 2016).

603 TOC ABSTRACT

604

605

